Thermal Analysis of Candidate Armor Materials for Use in the Magnetic Cusp Field HAPL Reactor Design

T.A. Heltemes, G.A. Moses

November 2006

UWFDM-1314

Presented at the 17th ANS Topical Meeting on Fusion Energy, 13-15 November 2006, Albuquerque NM.

FUSION TECHNOLOGY INSTITUTE

UNIVERSITY OF WISCONSIN

MADISON WISCONSIN

Thermal Analysis of Candidate Armor Materials for Use in the Magnetic Cusp Field HAPL Reactor Design

T.A. Heltemes, G.A. Moses

Fusion Technology Institute
University of Wisconsin
1500 Engineering Drive
Madison, WI 53706

http://fti.neep.wisc.edu

November 2006

UWFDM-1314

Presented at the 17th ANS Topical Meeting on Fusion Energy, 13-15 November 2006, Albuquerque NM.

Thermal Analysis of Candidate Armor Materials for use in the Magnetic Cusp Field HAPL Reactor Design

T.A. Heltemes[1], G.A. Moses[1]

[1]*University of Wisconsin Fusion Technology Institute, Madison, 1500 Engineering Drive, Madison WI, 53597*
taheltemes@wisc.edu

The introduction of magnetic cusp fields into the High Average Power Laser (HAPL) reactor design is to prevent target ions from interacting with the armor layer. Diverting the ions and preventing their impact on the chamber armor eases thermal design constraints considerably. The BUCKY code was used to simulate thermal loads for the candidate armor materials tungsten and silicon carbide.

Parametric analysis was done to ascertain the peak X-ray temperature rise in the armor due to X-rays from the HAPL target thermonuclear ignition. Temperature values as a function of chamber armor radius were obtained using initial conditions of T_0 = 600 ˚C and xenon buffer gas pressures of 66.7, 666.7 and 6666.1 mPa (0.5, 5 and 50 mTorr). The armor radius was decreased until thermal thresholds were met (2400 ˚C and 1000 ˚C for tungsten and silicon carbide, respectively) to determine the minimum allowable radius of the HAPL chamber.

A second set of parametric simulations were performed at xenon gas pressures of 666.7 and 6666.1 mPa (5 and 50 mTorr) to a time of 5 ms to observe the effect of re-radiation from the buffer gas on the surface temperature of tungsten and silicon carbide.

I. Introduction

The BUCKY 1-D radiation hydrodynamics code has been used for the simulation of both inertial confinement fusion (ICF) targets and reaction chambers (Ref. 1). This latter capability of the BUCKY code has been used to estimate the thermal response of the HAPL target chamber (Ref. 2) due to impinging ion and X-ray threat spectra (Ref. 3). These previous simulations have demonstrated BUCKY's capability to generate thermal profiles similar to those from other numerical techniques (Ref. 4).

These past simulations have used an idealized set of initial conditions for chamber temperatures and pressures (Ref. 4). This paper presents the results of simulations performed with the specific set of initial conditions proposed for the HAPL chamber (chamber initial temperature of 600˚C and 66.7 mPa (0.5 mTorr).

One proposed method for mitigating the heating effects of the ion threat spectra is through the introduction of a magnetic cusp field to divert the ions away from the wall (Ref. 5). In the absence of ions, the sole driving factor on the temperature response of chamber armor materials is through the deposition of X-ray energy. This paper examines how the minimum radius of the HAPL chamber may be decreased when cusp fields are used to divert the ions.

A method for mitigating the effect of both X-rays and ions is through increasing the pressure of the buffer gas in the chamber (Ref. 4). This paper addresses the effect of using an increased chamber gas pressure in conjunction with magnetic cusp field ion diversion.

II. BUCKY Simulation Parameters

II.A. HAPL Chamber Armor Parameters

Previous work using BUCKY has concentrated on using xenon as the chamber buffer gas and tungsten as the armor material covering the ferritic steel first wall (Ref. 4). This paper examines the effects of 1 cm silicon carbide armor in addition to 1 mm tungsten armor. Fig. 1 shows the temperature-dependent thermal conductivity of tungsten and silicon carbide. Fig. 2 shows the temperature-dependent specific heat of tungsten and silicon carbide. Dashed values are a linear extrapolation of the last available data point for each quantity.

The equations of state for the xenon and armor materials in the gas and plasma states were modeled using one-temperature SESAME data (Ref. 6). YAC local thermodynamic equilibrium (LTE) X-ray opacity data were used for the xenon and armor materials (Ref. 7).

II.B. X-ray and Ion Threat Spectra

These simulations use the ion and X-ray threat spectra emanating from the 365 MJ palladium and gold coated HAPL target. A LASNEX simulation performed at Lawrence Livermore National Laboratory (LLNL) was used to obtain the target spectra, which were reported at a time of 100 ns. (Ref. 3). Fig. 3 shows the radial build of

the target, fig. 4 shows the time-integrated X-ray threat spectrum and fig. 5 shows the time-integrated ion threat spectra. For the purposes of the simulation, all ions are launched into the buffer gas at $t = 0$ s and the X-rays threat spectra intensity is scaled by a time-dependent Gaussian function with a full-width half maximum (FWHM) of 170 ps.

III. Minimization of the HAPL Magnetic Cusp Field Chamber Radius

The BUCKY code does not inherently support the physics of ion deflection and removal from the simulation. The code was modified to remove ions before impacting the wall to simulate magnetic cusp field diversion. The ions were allowed to propagate freely through the simulation until they reached a point 25 cm from the wall. At the 25 cm threshold, the ion kinetic energy is zeroed out to represent diversion by the cusp field. The accounting routines already present in the BUCKY code to then removed the ions from the simulation. The ions were allowed to travel through the buffer gas so that they would deposit energy in the gas during transit, a process that becomes important to re-radiation from the buffer gas at high pressure (Ref. 8).

For each of the desired xenon buffer gas pressures — 66.7, 666.7 and 6666.1 mPa (0.5, 5.0 and 50.0 mTorr) — BUCKY simulations were performed with a chamber radius of 10.5 m (the HAPL standard chamber). The chamber radius was then reduced in 10 cm increments until the specified threshold temperatures were reached (2400 ˚C for tungsten and 1000 ˚C for silicon carbide). The peak temperature in the first 1×10^{-5} cm armor zone was reported for the parametric simulations. Fig. 6 shows the results of the tungsten simulations and fig. 7 shows the results of the silicon carbide simulations.

The peak temperature values were fit to a R^{-2} curve, yielding analytical expressions for the peak temperature at the surface of the armor as a function of chamber radius in meters. The equation is of the form

$$T(r) = C_1 r^{-2} + C_2 r^{-1} + C_3 \qquad (1)$$

where C_1, C_2 and C_3 are coefficients dependent on armor material and xenon gas pressure (Table I).

Using Eq. (1) with the coefficients found in Table I, the minimum chamber radius with a peak surface temperature of 2400˚C for tungsten and 1000˚C for silicon carbide were calculated. Table II shows the results of these calculations.

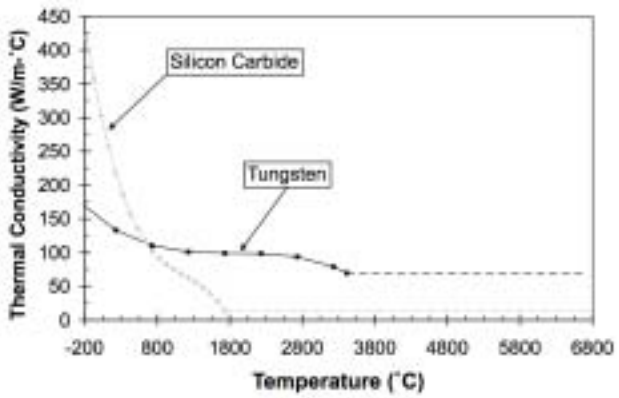

Fig. 1. Thermal conductivity of tungsten and silicon carbide.

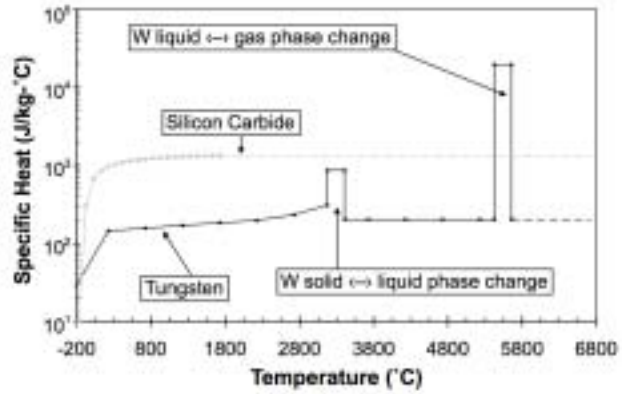

Fig. 2. Specific heat of tungsten and silicon carbide.

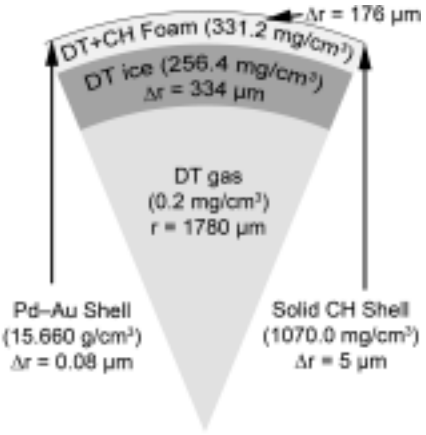

Fig. 3. 365 MJ HAPL target radial build.

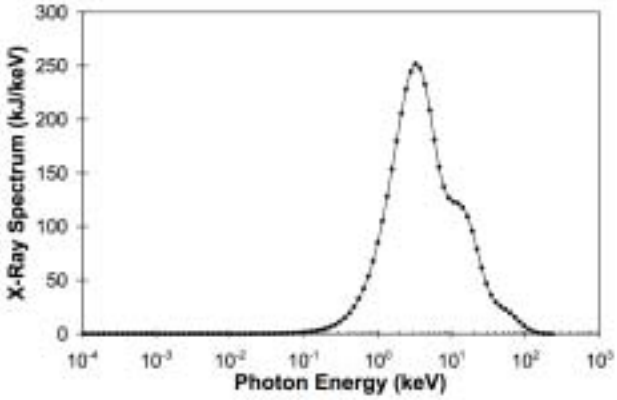

Fig. 4. 365 MJ HAPL target LASNEX X-ray spectrum at 100 ns.

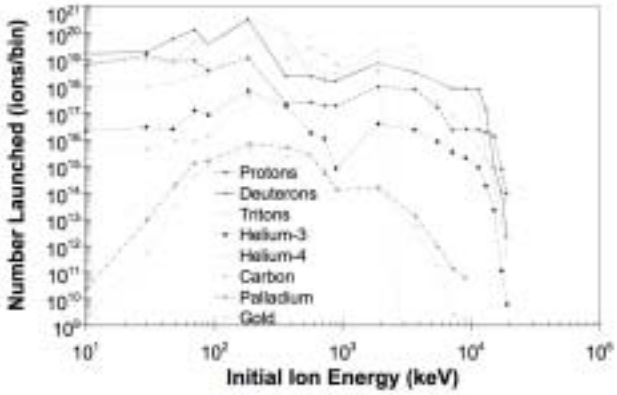

Fig. 5. 365 MJ HAPL target LASNEX ion spectra at 100 ns.

IV. Xenon Buffer Gas Effect on Minimization of the HAPL Magnetic Cusp Field Chamber

The minimum radius values from Table II and xenon buffer gas pressures can be used to construct a function that produces a minimum buffer gas pressure for a given chamber radius that will not exceed the temperature criteria of 2400˚C for tungsten and 1000˚C for silicon carbide. For tungsten armor, the minimum xenon gas pressure required for a desired chamber radius is given by

$$P(r) = -382.499 \log(r) + 301.740 \quad (2)$$

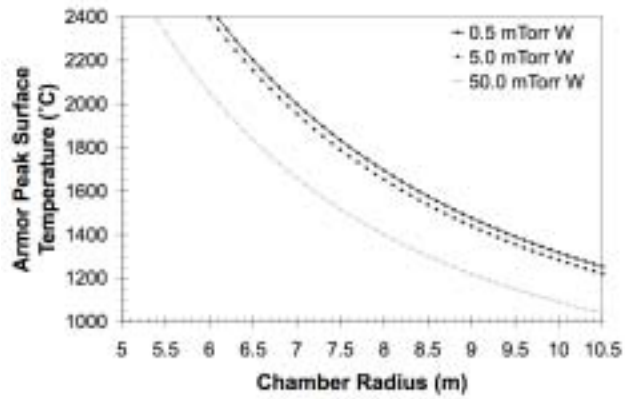

Fig. 6. Peak temperature in tungsten armor.

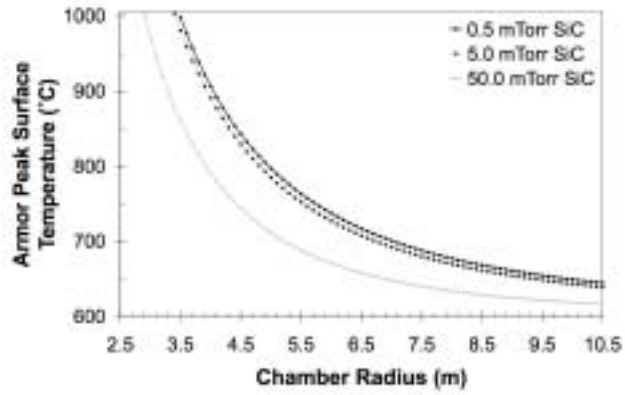

Fig. 7. Peak temperature in silicon carbide armor.

where r is the chamber radius in meters and $P(r)$ is the minimum required xenon gas pressure given in mTorr. For silicon carbide armor, the minimum xenon buffer gas pressure required for a desired chamber radius is given by

$$P(r) = -299.138 \log(r) + 163.787 \quad (3)$$

where r is the chamber radius in meters and $P(r)$ is the minimum required xenon gas pressure given in mTorr. The R^2 figures of merit are 0.998971 and 0.99833 for the tungsten and silicon carbide curve fits, respectively.

TABLE I. Peak Temperature Coefficients

Configuration	C_1	C_2	C_3
Tungsten & 66.7 mPa (0.5 mTorr) xenon	4.5957×10^{4}	4.7508×10^{3}	3.8211×10^{2}
Tungsten & 666.7 mPa (5.0 mTorr) xenon	4.6495×10^{4}	4.3488×10^{3}	3.8271×10^{2}
Tungsten & 6666.1 mPa (50.0 mTorr) xenon	3.4188×10^{4}	1.2344×10^{3}	4.7550×10^{2}
Silicon Carbide & 66.7 mPa (0.5 mTorr) xenon	4.6816×10^{3}	7.1560×10^{1}	5.9511×10^{2}
Silicon Carbide & 666.7 mPa (5.0 mTorr) xenon	4.6847×10^{3}	7.7135×10^{0}	5.9566×10^{2}
Silicon Carbide & 6666.1 mPa (50.0 mTorr) xenon	2.6773×10^{3}	-1.6708×10^{2}	6.0144×10^{2}

TABLE II. Minimum Chamber Radius

Configuration	Minimum Chamber Radius (m)
Tungsten & 66.7 mPa (0.5 mTorr) xenon	6.10
Tungsten & 666.7 mPa (5.0 mTorr) xenon	6.00
Tungsten & 6666.1 mPa (50.0 mTorr) xenon	4.55
Silicon Carbide & 66.7 mPa (0.5 mTorr) xenon	3.49
Silicon Carbide & 666.7 mPa (5.0 mTorr) xenon	3.42
Silicon Carbide & 6666.1 mPa (50.0 mTorr) xenon	2.40

V. Re-radiation Analysis of the HAPL Magnetic Cusp Field Chamber

Ions transiting the chamber gas are slowed through both electron and nuclear scattering. These scattering events deposit energy into the chamber gas and plasma. This energy is re-radiated by the chamber buffer gas on a long time scale compared to the X-rays emanating from the target burn. In order to investigate the effect of X-ray re-radiation from low-pressure xenon chamber buffer gas, a set of simulations was performed out to a time of 5 ms. The chamber radius for both armor materials was decreased in 0.5 m increments until the X-ray peak threshold temperature was met or exceeded. Fig. 8 shows the result of tungsten with 666.7 mPa (5.0 mTorr) xenon buffer gas. Fig. 9 shows the result of tungsten with 6666.1 mPa (50.0 mTorr) xenon buffer gas. Fig. 10 shows the result of silicon carbide with 666.7 mPa (5.0 mTorr) xenon buffer gas. Fig. 11 shows the result of silicon carbide with 6666.7 mPa (50.0 mTorr) xenon buffer gas.

Figs. 8–11 do not show any indication of temperature rise due to xenon buffer gas re-radiation at times of up to 5 ms from the point of target ignition. It was noted that the 666.7 mPa (5.0 mTorr) surface temperature shows a temperature "spike" at approximately 10–20 μs into the simulation. This spike was determined to be a numerical artifact of ions traveling over 25 cm in a single time step, interacting with the armor before the kinetic energy was zeroed out.

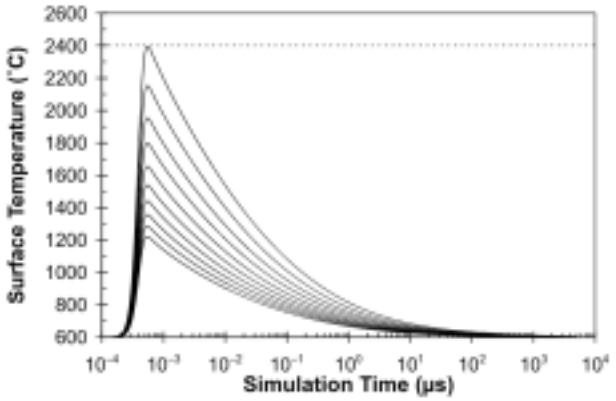

Fig. 8. Temperature rise on the surface of tungsten armor with 666.7 mPa (5.0 mTorr) xenon buffer gas.

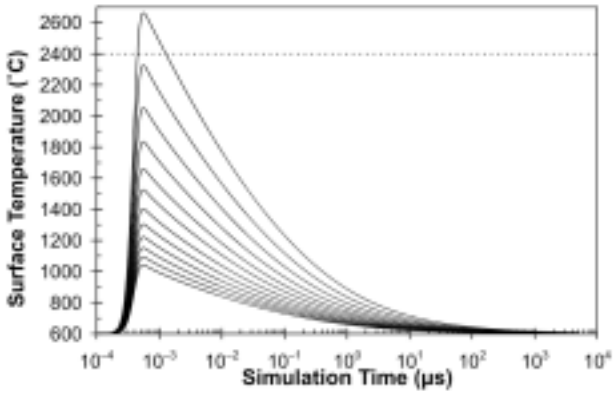

Fig. 9. Temperature rise on the surface of tungsten armor with 6666.1 mPa (50.0 mTorr) xenon buffer gas.

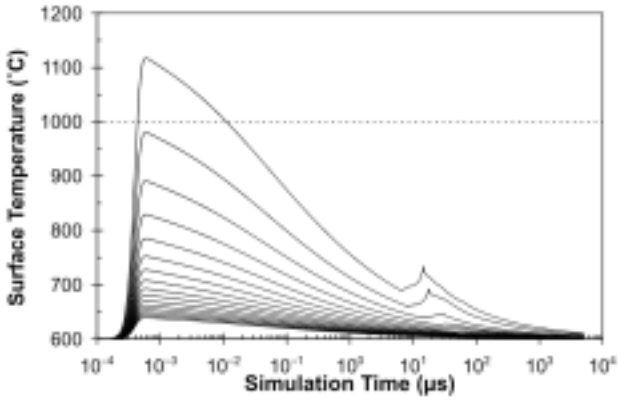

Fig. 10. Temperature rise on the surface of silicon carbide armor with 666.7 mPa (5.0 mTorr) xenon buffer gas.

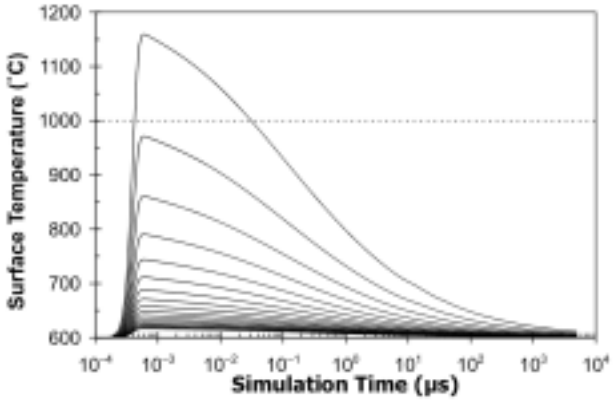

Fig. 11. Temperature rise on the surface of silicon carbide armor with 6666.1 mPa (50.0 mTorr) xenon buffer gas.

VI. CONCLUSIONS

The BUCKY 1-D radiation hydrodynamics code was used to study the effect of implementing a magnetic cusp field diverter on the HAPL chamber design. Parametric analysis was performed to determine the peak surface temperature of the chamber armor at xenon buffer gas pressures of 66.7 mPa, 666.7 mPa and 6666.1 mPa (0.5 mTorr, 5.0 mTorr and 50.0 mTorr) as the chamber radius was decreased in 10 cm increments.

Curve fit equations were developed to estimate the minimum chamber radii at the constraining surface temperatures of 2400˚C and 1000˚C for tungsten and silicon carbide armors, respectively. A second set of curve fit equations was developed to ascertain the effect of increasing buffer gas pressure on the minimum allowable chamber radii. The results of this analysis indicates that magnetic cusp field diversion of the target ions allows for a significant decrease in chamber radius, especially in conjunction with the presence of a low to moderate xenon buffer gas to mitigate X-ray energy deposition in the armor material.

5 ms BUCKY simulations were performed with xenon buffer gas pressures of 666.7 mPa and 6666.1 mPa (5.0 mTorr and 50.0 mTorr) to examine the effect of re-radiation from the xenon buffer gas on the surface of the armor materials over a long time interval. The results of these simulations indicate that re-radiation plays no appreciable role on surface temperatures for buffer gas pressures up to 6666.1 mPa (50.0 mTorr).

ACKNOWLEDGMENTS

This work was supported in part by a grant from the Naval Research Laboratory, award no. N00173-03-1-G901. The authors wish to thank Dr. Robert R. Peterson of Los Alamos National Laboratory for his ongoing support and advice regarding the improvement of the BUCKY simulation models.

REFERENCES

1. R.R. Peterson, J.J. MacFarlane, G.A. Moses, “BUKCY—A 1-D Radiation Hydrodynamics Code for Simulating Inertial Confinement Fusion High Energy Density Plasmas,” *UWFDM-984*, University of Wisconsin (1995).
2. Available online at http://www.aries.ucsd.edu/HAPL/DOCS/example.html
3. Available online at http://www.aries.ucsd.edu/HAPL/DOCS/HAPLtargetSpecs.pdf
4. T.A. Heltemes, D.R. Boris, G.A. Moses and M. Fatenejad, “Simulation of thermal response and ion deposition in the HAPL target chamber 1 mm tungsten armor layer using the improved BUCKY code,” *Fusion Engineering and Design*, In Press, Corrected Proof, Available online 13 October 2006, http://www.sciencedirect.com/science/article/B6V3C-4M3RP69-1/2/173c331e676db0368a72b2626d444c71
5. A.R. Raffray, J. Blanchard, A.E. Robson, D.V. Rose, M. Sawan, J. Sethian, L. Snead, I. Sviatoslavsky and the HAPL Team, “Impact of Magnetic Diversion on Laser IFE Reactor Design and Performance,” *Proc. Inertial Fusion Sciences and Applications (IFSA 2005)*, Biarritz, France, Sept. 4–9, 2005, **133** p. 845, *J. Phys. IV France* (2006).
6. B.I. Bennet, J.D. Johnson, G.I. Kerley, G.T. Rood, “Recent Developments in the SESAME Equation-of-State Library,” Los Alamos National Laboratory, NM, LA-7130 (1978).
7. J. Yuan, D.A. Haynes, R.R. Peterson, G.A. Moses, “Flexible database-driven opacity and spectrum calculations,” *J. Quant. Spect. Rad. Trans.* **81**, 513 (2003).
8. R.R. Peterson, C.L. Olson, T.J. Renk, G.E. Rochau and M.A. Sweeney, “Chamber dynamic research with pulsed power,” *Nuclear Instruments and Methods in Physics Research Section A: Accelerators, Spectrometers, Detectors and Associated Equipment*, **464**, *1–3*, 172 (2001).